

## RBS AND TEM STUDIES OF INDIUM PHOSPHIDE IRRADIATED WITH 100 keV Au IONS

*A. S. Khalil*<sup>a,1</sup>, *A. Yu. Didyk*<sup>b,2</sup>

<sup>a</sup> Tabbin Institute for Metallurgical Studies, Cairo, Egypt

<sup>b</sup> Joint Institute for Nuclear Research, Dubna

Transmission Electron Microscopy (TEM) and Rutherford Backscattering (RBS) have been used to observe the spatially isolated disordered zones in InP resulting from 100 keV Au ion irradiation at room temperature. Studies were carried out in interval of irradiation fluences less than lower value of full amorphization fluence. Such a value of fluence, as was established in the studies, can be estimated of order  $\sim 2.5 \cdot 10^{13} \text{ cm}^2$ . The accumulation of damage due to the 100 keV Au ion irradiation was described in this material using a composite theoretical model accounting for both homogeneous and heterogeneous amorphization processes.

Методы просвечивающей электронной микроскопии (ПЭМ) и резерфордовского обратного рассеяния (РОР) были использованы для изучения частично изолированных разупорядоченных областей в образцах InP, облученных при комнатной температуре ионами золота с энергией 100 кэВ. Исследования проводились в интервале значений флюенсов, меньших значений флюенса, начиная с которого происходит полная аморфизация образцов InP. Нижнее значение этого флюенса, как было установлено, составляет  $\sim 2,5 \cdot 10^{13} \text{ см}^{-2}$ . Процессы накопления дефектов структуры были описаны с использованием объединенной модели, учитывающей как однородный, так и гетерогенный процессы аморфизации.

PACS: 34.50.-s; 61.80Lj; 61.80.-x

### INTRODUCTION

The formation of spatially isolated disordered and/or amorphous zones by low-energy heavy-ion irradiation in semiconductor materials and their subsequent electron irradiation-induced recovery (annealing) have recently received much attention [1]. Both fundamental and technological insights are gained by investigating the evolution of these zones as they represent the precursor structures from which a continuous amorphous layer is formed in implanted semiconductor devices when the irradiating ion fluences reach levels to cause complete amorphization of top layer. Molecular dynamics simulations and other theoretical investigations of the damage caused by energetic heavy ion implanted in semiconductor substrates have revealed that a characteristic feature is the presence of disordered/amorphous zones created by the release of large amount of kinetic energy in local regions [2]. These zones can account for part or most of the produced damage in the irradiated material, the

---

<sup>1</sup>E-mail: askhali2004@yahoo.com

<sup>2</sup>E-mail: didyk@jinr.ru

extent of which depends on the crystal structures and bond strengths of target material. Thus, as the ion fluences increase, these zones overlap until a continuous amorphous layer is formed.

Since the first direct TEM observation of disordered zones in an irradiated elemental semiconductor by Parsons et al. [3], many TEM investigations have been performed. An extensive TEM investigation of isolated disordered zones in Si and Ge has been described by Howe et al. [4]. In their investigations, irradiations were performed at low temperatures  $T < 50$  K using a range of heavy ions from  $P^+$  to  $Bi^+$  ions into Si and from  $As^+$  to  $Bi^+$  ions into Ge at energies between 10 and 120 keV. For heavier ions, the diffraction contrast of zones observed in the TEM was stronger than that for lighter ions, which may be explained by the denser cascades in the case of heavier ions. From diffraction contrast experiments, it was concluded that the damage could be *best* described as amorphous in nature. In another study, high resolution transmission electron microscopy (HRTEM) observation of heavy ion irradiated Si at 4 K by Narayan et al. [5] revealed that the damaged zones were *indeed* amorphous in nature. In contrast, Howe and Rainville [6] simply suggested that the damage level in the peripheral regions of the zones had simply become large enough to produce diffraction contrast observed by TEM. The HRTEM by Ruault et al. [7] was used to investigate individual zones in 50–200 keV  $Bi^+$  ion irradiated Si. They noted that the core was amorphous in nature (see track model developed in [8]). The TEM observation revealed that core diameters were not sufficiently large to explain the formation of an amorphous layer at fluences  $\sim 6.0 \cdot 10^{12} \text{ cm}^{-2}$ . In-situ observations showed that when the ion fluence was increased and strongly contrasting damaged regions began to overlap, additional regions appeared with characteristic weaker contrast than that exhibited by the damaged cores produced in completely isolated zones. It was suggested that the overlap of these weaker contrast damaged regions outside the amorphous cores was responsible for the progression of amorphization. These regions, termed *gray* zones, first began to appear in the area between existing strong contrasts regions [9]. At higher fluences both the strong dark contrast defects and the gray zones increasingly overlapped. The authors conclude that gray zones represent a separate amorphous state distinct from the amorphous zones themselves inside the cores and that these play some part in the total amorphization process, although no satisfactory explanation is given to support this idea. However, in an earlier observation by Chadderton [10] in 100–400 keV  $Bi^+$  irradiated Si, it was found that for irradiation at room temperature, *some* but not all of the observed disordered zones could be described as amorphous. In the case of compound semiconductors irradiated with heavy ions, we cite the earlier work of Chandler and Jenkins [11] and especially the work of Jenkins [12] on 100 keV irradiation of different heavy-ion species into the compound semiconductors GaAs and GaP. *Spot* damage was observed in GaP which exhibited the same structure factor contrast as Si and Ge. The defect yield, defined as the ratio of the ion fluence to the observed zone density, was close to unity for all ion damage in GaP, and the average diameter of the damaged regions was about several nanometers. These observations led to the conclusion that zones in GaP were amorphous. In comparison, the damage in GaAs consisted of a very low density of weak TEM contrast features that could not be identified unambiguously. In the case of InP, spatially isolated zones in InP irradiated with 50 keV  $Si^+$  ions at room temperature were investigated using TEM [13]. A diffuse ring characterizing the onset of amorphization appeared in the electron diffraction pattern at irradiation fluences  $\sim 2.0 \cdot 10^{13} \text{ cm}^{-2}$ . Complete amorphization was ascribed to the previously mentioned overlap of the gray zones as for the case of the irradiated elemental semiconductor Si advocated by

the same investigators [7, 14]. An important observation was that these zones were found to shrink and disappear during prolonged TEM observation at electron beam energies  $\geq 100$  keV at room temperature [13]. More recent TEM observations of isolated zones following ion irradiation have been reported in the compound semiconductors GaAs, GaP, InP (in addition to the elemental semiconductors Si and Ge) [1, 5, 15, 16–21]. However, the authors assumed that the observed zones in *all* the compound and elemental semiconductors investigated were amorphous in nature, based on TEM observations of zones for *only* GaAs irradiated with heavy ions [22] which appear as dark contrast irregular features in conventional TEM.

In the present investigation, we further investigate the formation and accumulation of point defects and creation of disordered zones produced by low-energy Au<sup>+</sup> ion irradiation in InP has been followed by TEM observation and RBS/C analysis.

## 1. EXPERIMENTAL STUDIES

InP samples were prepared for irradiation from a 500  $\mu\text{m}$  thick, semi-insulating, polished, (001) oriented InP wafer; each bulk sample being scribed and cut into pieces of  $\sim 10 \times 10$  mm for ion irradiation. In addition to bulk samples, thin foil samples (electron transparent  $\leq 200$  nm thick) were prepared before the ion irradiation in order to avoid the artifacts usually associated with post-irradiation preparation of InP and to facilitate the immediate TEM observation of the irradiated samples. The thin foils were prepared by first coring 3 mm disks from slivers of the (001) InP wafer. The disks were then mechanically ground and dimpled to a thickness of 100  $\mu\text{m}$  before being chemically thinned to perforation in 2% bromine-methanol solution. Both the bulk and thin foil samples were irradiated with 100 keV Au<sup>+</sup> ions in a non-channelling direction at room temperature using the tandem accelerator at the Electronic Materials Engineering Department of the Australian National University (ANU). The ion fluence ranged from  $1.0 \cdot 10^{12}$ – $1.0 \cdot 10^{14}$   $\text{cm}^{-2}$  and the ion flux was  $\sim 5.7 \cdot 10^{11}$   $\text{cm}^{-2} \cdot \text{s}^{-1}$ . Subsequently the irradiated bulk samples were analyzed by Rutherford backscattering with 2 MeV He<sup>+</sup> ions, and a glancing scattering angle of  $\sim 120^\circ$ .

TEM studies were carried out on transmission electron microscope Philips CM-300. Electron beam energy can be varied from 100 to 300 keV with the current density in the range  $0.1 \leq J \leq 0.4$  A/cm<sup>2</sup>. During electron irradiation the electron beam was spread over a radius  $\sim 1.5$ – $2$   $\mu\text{m}$ .

## 2. RESULTS AND DISCUSSION

Isolated disordered zones visible in the TEM display a characteristic contrast. These zones appear in the TEM as dark irregular features of different sizes distributed over the irradiated area. Figure 1 shows these characteristic spot contrast in 100 keV Au<sup>+</sup> ion irradiated InP. The micrograph was obtained under BF conditions along the  $\langle 001 \rangle$  zone axis, chosen so as to improve both resolution and contrast [23, 24]. An image of an unirradiated sample is shown for comparison, displaying only the observed simple extinction contours where regions of the crystal satisfy the Bragg condition for the imaging electrons. The contrast is similar to that observed in other irradiated compound semiconductor materials [1], where the irregular strain contrast observed by TEM maps the boundary of a three-dimensional disordered zone.

The contrast arises predominantly from strain in the lattice surrounding the damaged «core» resulting from a cascade which might, for example, contain a distribution of point defects or point defect clusters and/or amorphous material. This lattice disorder and associated strain-fields scatters (diffracts) illuminating electrons which give rise to the dark features observed in BF-TEM. Diffraction patterns (inset in Fig. 1, *b*) observed at these relatively low ion fluences ( $1.0 \cdot 10^{12} \text{ cm}^{-2}$ ) exhibit the sharp spots associated with unirradiated InP, there

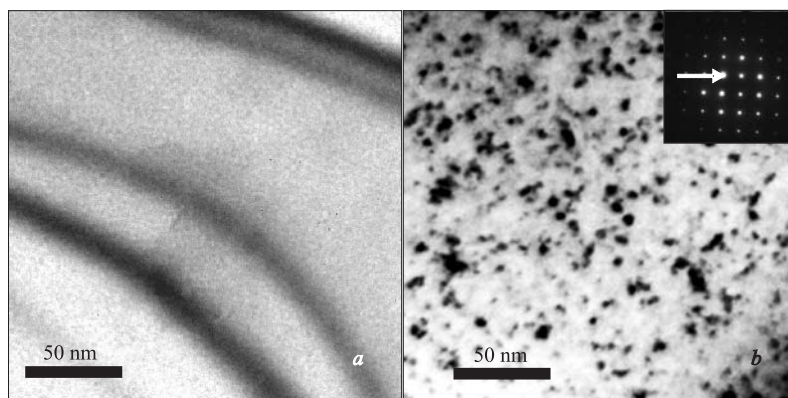


Fig. 1. BF-TEM of (*a*) sample before irradiation and (*b*) residual disorder following 100 keV Au<sup>+</sup> ( $1.0 \cdot 10^{12} \text{ cm}^{-2}$ ) irradiation in InP imaged along [001] zone axis orientation (in the SADP inset the arrow points to the transmitted «undiffracted» beam)

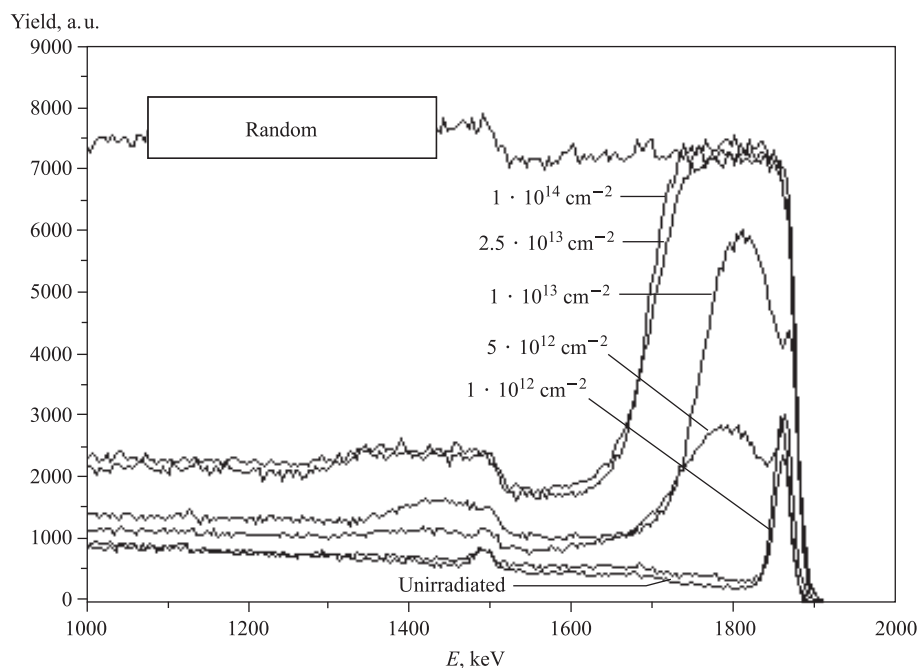


Fig. 2. RBS/C spectra of 100 keV Au<sup>+</sup> irradiated InP for different ion fluences

were no rings, diffuse or otherwise. Given that the total volume of the defective material is relatively small compared to the intact surrounding matrix, it is possible that they might indeed be amorphous and the rings simply too diffuse to be detectable. The possibility that the disordered zones might be simply an agglomeration of point defects and not amorphous in nature or a combination of both must be considered. In Fig. 2, a sequence of RBS/C spectra is presented for InP samples irradiated with 100 keV Au<sup>+</sup> ions up to a fluence of  $1.0 \cdot 10^{14} \text{ cm}^{-2}$ . It should be noted that there exists a minimum between the surface peak and the damage peak which persists, even for fluences between  $5.0 \cdot 10^{12}$  and  $1.0 \cdot 10^{13} \text{ cm}^{-2}$ . This implies that damage is relatively low and that some crystallinity remains for this depth. For the sample irradiated to  $1.0 \cdot 10^{12} \text{ cm}^{-2}$ , the RBS/C spectrum shows that the amount of damage is noticeably low compared to higher fluences and is barely distinguishable from the unirradiated sample. However, the damage at this relatively low fluence is clearly evident as disordered zones which are revealed by TEM (Fig. 1). This indicates the higher relative sensitivity and the merit of TEM analysis at lower irradiation fluence regimes when compared to RBS/C analysis.

The RBS/C yield increases with increasing fluence are consistent with an increase in disorder build-up in InP. When the irradiated InP becomes completely amorphous, the yield generally arrives at the random level. Thus, at fluences  $\sim 2.5 \cdot 10^{13} \text{ cm}^{-2}$  the backscattered spectrum has reached the random level indicating that the surface layer is amorphized.

The thickness of the amorphous layer was calculated to be  $(45 \pm 5) \text{ nm}$ . This is in a reasonable agreement with the value of  $R_p + \Delta R_p = 36.4 \text{ nm}$  (where  $R_p = 26.3 \text{ nm}$  is the 100 keV Au<sup>+</sup> ion range in InP and  $\Delta R_p = 10.1 \text{ nm}$  is the longitudinal straggling calculated from SRIM [25] simulations of 100 keV Au<sup>+</sup> ions into InP).

The mechanism of damage accumulation can be better understood by analyzing the fluence dependence of the lattice disorder measured by RBS/C. However, an accurate determination of the structure or atomistic nature of the He<sup>+</sup> scattering centres in the form of disordered zones is difficult, precisely because RBS/C is far less sensitive than TEM for revealing such damage at low fluence irradiation. The processes by which damage accumulates toward the eventual formation of an amorphous layer in semiconductors have been generally described by defect overlap models based on statistics describing the ratio of the surface area covered by ion irradiation damage to the total area being irradiated [28]. These damage build-up models usually lie between the limiting extremes of two basic mechanisms defining two categories of amorphization process [26] as shown in the inset in Fig. 3.

In the first, homogeneous nucleation (defect accumulation), amorphization occurs by the interaction and accumulation of simple point defects produced by irradiation until the defect density in a region of the irradiated lattice is so great that the region becomes unstable and spontaneously collapses to an amorphous state. In the second, heterogeneous nucleation (direct impact amorphization), small regions are directly amorphized during individual collision cascades and complete amorphization occurs by the accumulation and overlap of these regions. A detailed discussion and survey of various models can be found in reference [27].

Generally, amorphization in semiconductors can best be described by a combination of both heterogeneous and homogeneous mechanisms. Composite models have been developed wherein an impinging ion can produce both a combination and coexistence of both point defects and amorphous zones which, when overlapping, convert to the amorphous state [27]. The relative amount of damage as a function of fluence in 100 keV Au<sup>+</sup> ion irradiated

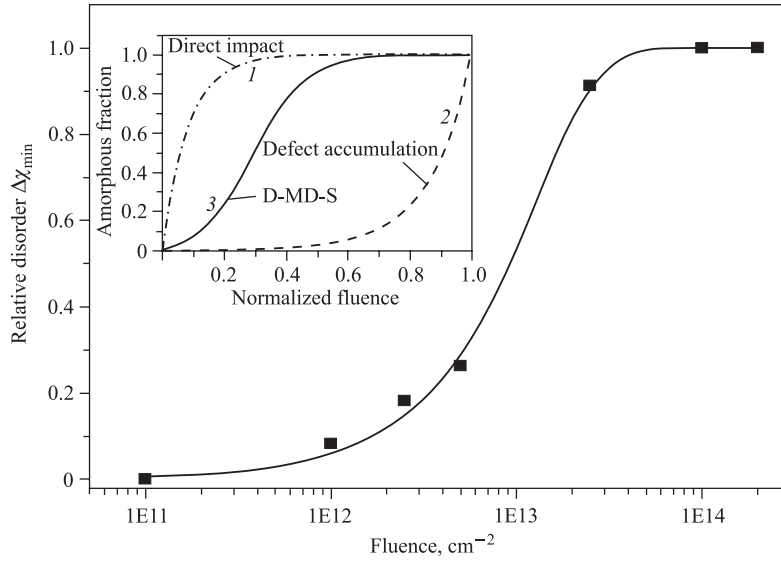


Fig. 3. A plot of relative disorder  $\Delta\chi_{\min}$  versus ion fluence for 100 keV  $\text{Au}^+$  ion irradiated InP. The best fit is obtained by using the modified Hecking model. The uncertainty for each ordinate data point is  $\leq 5\%$ . Inset graph is an idealized plot of the general three routes leading towards heavy ion-induced amorphization in materials; the direct impact (heterogeneous; 1), stimulated defect accumulation (homogeneous; 2) and a combination of both direct impact and stimulated defect accumulation (3)

InP can be extracted from the RBS/C yield ( $Y$ ); this is expressed as the relative disorder  $\Delta\chi_{\min}$  defined as

$$\Delta\chi_{\min} = \frac{Y_{\text{irrad}} - Y_{\text{unirrad}}}{Y_{\text{random}} - Y_{\text{unirrad}}}. \quad (1)$$

In this case, the value of  $\Delta\chi_{\min}$  expresses the relative amount of disorder in the crystal and approaches unity for complete amorphization at a fluence of  $\sim 2.5 \cdot 10^{13} \text{ cm}^{-2}$ . The  $\Delta\chi_{\min}$  calculated over the energy range of 1750–1850 keV (from Fig. 2) is plotted as a function of ion fluence in Fig. 3. Here we invoked Weber's expansion of the Hecking model for the accumulation of damage [27,28] as a realistic description of the amorphization process. In this model for description of damage accumulation an analytical expression is derived for the progression of amorphization which takes into account both types of damage. Thus, on the one hand, amorphization occurs heterogeneously (direct impact, i.e., each ion creates an amorphous zone) with probability  $P_a$ , and cross section for amorphization  $\sigma_a$  and  $f_a$  is the fraction of amorphous material. And on the other hand, taking into account homogeneous damage growth which is described by the overlap of pre-existing disorder (stimulated disorder, i.e., ions creates an ensemble of point defects) with a stimulated defect production probability  $P_s$  and cross section for stimulated amorphization  $\sigma_s$ . The probability  $P_i(f_a)$  for the amorphization process to occur is taken to be  $f_a(1 - f_a)$ . This direct-impact/defect-stimulated model is generally expressed as

$$\frac{df_a}{dF} = P_a(1 - f_a) + P_s f_a(1 - f_a). \quad (2)$$

The solution of the above equation (2) is expressed as follows:

$$f_a = 1 - (\sigma_a + \sigma_s) / (\sigma_s + \sigma_a \exp[\sigma_a + \sigma_s] F), \quad (3)$$

where  $F$  is the irradiating ion fluence.

From RBS/C spectra in Fig. 2, the best fit parameters for the plot of  $\Delta\chi_{\min}$  versus ion fluence (i.e., Eq. (3)) as shown in Fig. 3 are

$$\sigma_a = (5.99 \pm 0.64) \cdot 10^{-14} \text{ cm}^2 \text{ and } \sigma_s = (5.91 \pm 2.13) \cdot 10^{-14} \text{ cm}^2, \quad (4)$$

with almost equal weights for both cross sections, suggesting a real role for *both* processes for damage build-up. The importance of both processes was also confirmed by recent MD simulations of primary damage for several elemental and compound semiconductors [29], the radiation damage due to a single ion can comprise either amorphous or disordered zones with point defects intimately involved; i.e., both heterogeneous and homogeneous nucleation processes actually coexist. Amorphization, however, is not necessarily a simple phenomenon. Even if direct amorphization were to take place solely by means of heterogeneous nucleation [26] about the point at which each ion is ballistically stopped, factors such as point defects migration and recombination, local stoichiometric imbalance, dynamic annealing, the presence of impurities, sink effects such as surfaces, and the structure and variation of individual cascade damage can all play an important part. Furthermore, defects smaller than those resolved by TEM, point defects for example, can play a significant role in the amorphization process [29]. From the TEM analysis of zones at the lowest irradiation fluence ( $1.0 \cdot 10^{12} \text{ cm}^{-2}$ ), we have determined the size distribution of these zones as shown in Fig. 4. The data shown in Fig. 4 were obtained using the AnalySIS<sup>®</sup>, Soft Imaging System [25] determined by assuming that the area of each disordered zone is equivalent

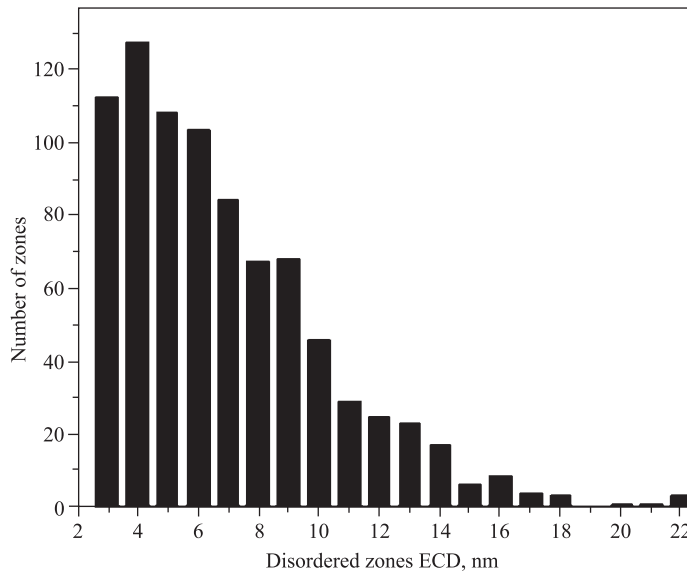


Fig. 4. Measured sizes of disordered zones in 100 keV  $\text{Au}^+$  ion irradiated InP at a fluence of  $1.0 \cdot 10^{12} \text{ cm}^{-2}$

to the area of a circle, therefore calculating the diameter of the corresponding circle expressed as an Equivalent Circle Diameter (ECD) in nanometers where  $ECD = 2\sqrt{A/\pi}$ , where  $A$  is the area of a zone. These results were determined from a micrograph over a total area of  $600 \times 600$  nm. Disordered zones  $\sim 2$  nm in diameter or less could not be unambiguously resolved due the finite resolution of the TEM. Also smaller radii would be physically meaningless, even if we were to assume that they are completely amorphous, given a minimum size requirement over which to define an amorphous phase within a crystalline lattice [30]. In addition, a difficulty is presented by defining the amorphous phase in InP where the complex nature of the amorphous phase can encompass a multitude of configurations which have been either theoretically predicted or experimentally verified, which include coordination numbers ranging from three to six atoms and homopolar bonding of both In and P atoms [31]. However, we found that the density of these zones is less than the ion fluence.

Thus, the density of TEM observed zones  $\sim 0.2$  of the corresponding ion fluence ( $1.0 \cdot 10^{12} \text{ cm}^{-2}$ ). An analogous yield (the areal density of zones per ion fluence) of less than unity ( $\sim 0.4\text{--}0.5$ ) for InP in-situ irradiated with 50 keV  $\text{Si}^+$  ions was also reported for irradiations both at room temperature and at 15 K [32]. This reported discrepancy between ion fluence and zone density does not suggest that this is due to an annealing process as it was carried out at very low temperature, but rather points to a strong probability for the existence of clusters which are not resolved by TEM. Similar observations for reduced defect yield were reported for 50 keV  $\text{Kr}^+$ ,  $\text{Xe}^+$  and  $\text{Au}^+$  ion irradiation at 30 K in GaAs and GaP [35]. This also may further point to the necessity of a coexistence of homogeneous nucleation mechanism and the subsequent overlap of disordered zones for complete amorphization, and that large proportion of damage might not be observed by TEM and that the observed zones are not necessarily amorphous in nature. Also, it should be emphasized that the energy loss process of an ion in the lattice is a statistical process and corresponds to the average over a series of single-energy-loss events. Therefore, it may be that not all the created damage can be resolved by TEM observation as each impinging 100 keV  $\text{Au}^+$  ion can create simple point defects and/or defect clusters which are certainly not resolved by TEM or it can create damage in the form of disordered zones  $\leq 1$  nm in size but which cannot be discerned by TEM observation. In addition, the action of surfaces as sinks for formed cascade defects must not be excluded. Furthermore, given the possibility of some overlap of zones at this ion fluence of  $1.0 \cdot 10^{12} \text{ cm}^{-2}$ , thus fluctuations in size and distribution of sizes of disordered zones are then unsurprisingly expected. Indeed, some observed zones are large and can reach 20 nm in diameter or more. However, the concentration of zones with small diameters (i.e., in the range  $\sim 3\text{--}8$  nm) is largest and the distribution is weighted towards smaller sizes, consistent with a theoretical study of size distribution of individual disordered and amorphous zones formation in semiconductors [34]. It must also be emphasized that zones *should* have a size distribution which can be wide and that variation in size is expected. This is more realistic than assigning only one value for heavy ion damage for the specified irradiation conditions as most models infer from the RBS/C measurements and the consequent modelling of the damage accumulation. We note here an observation made for medium-mass ion (300 keV  $\text{Si}^+$  and 600 keV  $\text{Se}^+$ ) irradiated InP [35]. However, in this work the authors used the simplest overlap Gibbons model [28] and inferred that overlap of zones is necessary for the creation of maximum damage in the form of completely amorphous layer [36].

## CONCLUSIONS

The damage created in InP single crystals by 100 keV Au<sup>+</sup> ions in the form of disordered zones for low-fluence ion irradiation was observed by TEM. These zones are characterized by an irregular shape and distribution in sizes, and their density is lower than the ion fluence. The exact atomistic nature of damage inside these zones cannot be determined unambiguously either by TEM or RBS/C. The damage increases with ion fluence until complete amorphization is reached at ion fluences  $\geq 2.5 \cdot 10^{13} \text{ cm}^{-2}$ . The best fit for the relative disorder induced by 100 keV Au<sup>+</sup> ion irradiation of InP from the RBS/C yields was obtained using the modified Hecking model which takes into account both heterogeneous (direct impact) and homogeneous (defect stimulated) amorphization. Thus, damage accumulation is best described by the invocation of both coexisting heterogeneous and homogeneous nucleation processes in low energy heavy ion irradiated InP.

## REFERENCES

1. Jencic I., Hollar E. P., Robertson I. M. Crystallization of Isolated Amorphous Zones in Semiconductors // *Philos. Mag.* 2003. V. 83. P. 2557–2571.
2. De la Rubia T. D. Irradiation-Induced Defect Production in Elemental Metals and Semiconductors: A Review of Recent Molecular Dynamics Studies // *Ann. Rev. Mater. Sci.* 1996. V. 26. P. 613–649.
3. Parsons J. R., Balluffi R. W., Koehler J. S. Direct Observation of Neutron Damage in Germanium // *Appl. Phys. Lett.* 1962. V. 1. P. 57.
4. Howe L. M., Rainville M. H. Heavy Ion Damage in Silicon and Germanium // *Nucl. Instr. Meth. B.* 1987. V. 19/20. P. 61.
5. Narayan J. et al. High-Resolution Imaging of Ion-Implantation Damage and Mechanism of Amorphization in Semiconductors // *Mater. Lett.* 1984. V. 2(3). P. 211–218.
6. Howe L. M., Rainville M. H. Features of Collision Cascades in Silicon as Determined by Transmission Electron Microscopy // *Nucl. Instr. Meth.* 1981. V. 182/183. P. 143.
7. Ruault M. O. et al. High Resolution and In-situ Investigation of Defects in Bi-Irradiated Si // *Philos. Mag. A.* 1984. V. 50(5). P. 667–675.
8. Didyk A. Yu., Varichenko V. S. Track Structure in Dielectric and Semiconductor Single Crystals Irradiated by Heavy Ions with High Level Inelastic Energy Losses // *Nucl. Track Rad. Meas.* 1995. V. 25, No. 1–4. P. 119–124.
9. Bernas H., Ruault M. O., Zheng P. Multiple Amorphous States in Ion Implanted Semiconductors Si and InP // *Cruc. Iss. Semicond. Mater. Proces. Techn. / Ed. Coffa S. Kluwer Acad. Publ.*, 1992.
10. Chadderton L. Nucleation of Damage Centers during Ion Implantation of Silicon // *Rad. Eff.* 1971. V. 8. P. 77–86.
11. Chandler T. J., Jenkins M. L. The Structure of Displacement Cascades in III-V Semiconductors // *Microscopy of Semiconductor Materials. Ser. 67. Inst. of Phys. Conf. London*, 1983.
12. Jenkins M. L. et al. In-situ Observations of the Development of Heavy-Ion Damage in Semiconductors // *Microscopy of Semiconductor Materials. Ser. 79. Inst. of Phys. Conf. London*, 1985.

13. Zheng P. *et al.* In-situ Defect Studies on Si Implanted InP // *J. Phys. D.* 1990. V. 23. P. 877–883.
14. Ruault M. O., Chaumont J., Bernas H. Transmission Electron Microscopy Study of Ion Implantation Induced Si Amorphization // *Nucl. Instr. Meth.* 1983. V. 209/210. P. 351–356.
15. Jencic I., Robertson I. M. Low-Energy Electron Beam Induced Regrowth of Isolated Amorphous Zones in Si and Ge // *J. Mater. Res.* 1996. V. 11(9). P. 2152–2157.
16. Jencic I., Hollar E. P., Robertson I. M. Electron-Induced Regrowth of Isolated Amorphous Zones in GaAs // *Nucl. Instr. Meth. B.* 2001. V. 175. P. 197–201.
17. Robertson I. M., Jencic I. Regrowth of Amorphous Regions in Semiconductors by Sub-Threshold Electron Beams // *J. Nucl. Mater.* 1996. V. 239(1–3). P. 273–278.
18. Bench M. W. *et al.* Production of Amorphous Zones in GaAs by the Direct Impact of Energetic Heavy Ions // *J. Appl. Phys.* 2000. V. 87(1). P. 49–56.
19. Jencic I. *et al.* Computer Image Analysis of Shrinkage of Isolated Amorphous Zones in Semiconductors Induced by Electron Beam // *Nucl. Instr. Meth. B.* 2002. V. 186. P. 126–131.
20. Jencic I., Robertson I. M. Regrowth of Heavy-Ion Implantation Damage by Electron Beams // *Mater. Sci. Semicond. Proces.* 2000. V. 3(4). P. 311–315.
21. Jencic I., Robertson I. M., Skvarc J. Electron Beam Induced Regrowth of Ion Implantation Damage in Si and Ge // *Nucl. Instr. Meth. B.* 1999. V. 148(1–4). P. 345–349.
22. Jencic I. *et al.* Electron-Beam-Induced Crystallization of Isolated Amorphous Regions in Si, Ge, GaP and GaAs // *J. Appl. Phys.* 1995. V. 78(2). P. 974–982.
23. Jenkins M. L., Kirk M. A. Characterization of Radiation Damage by Transmission Electron Microscopy // Ser. «Microsc. Mater. Sci.». Inst. of Phys. London, 2001.
24. Bench M. W., Tappin D. K., Robertson I. M. On the Suitability of the Down-Zone Imaging Technique to the Study of Radiation Damage // *Philos. Mag. Lett.* 1992. V. 66(1). P. 39–45.
25. AnalySIS<sup>®</sup>. Soft Imaging System. <http://www.soft-imaging.net>
26. Gibbons J. F. Ion Implantation in Semiconductors: II. Damage Production and Annealing // *Proc. of the Inst. of Electrical and Electronics Engin.* 1972. V. 60(9). P. 1062–1096.
27. Weber W. J. Models and Mechanisms of Irradiation-Induced Amorphization in Ceramics // *Nucl. Instr. Meth. B.* 2000. V. 166/167. P. 98–106.
28. Hecking N., Heidemann K. F., Kaat E. T. Model of Temperature Dependent Defect Interaction and Amorphization in Crystalline Silicon during Ion Irradiation // *Nucl. Instr. Meth. B.* 1986. V. 15. P. 760–764.
29. Nord J., Nordlund K., Keinonen J. Amorphization Mechanism and Defect Structures in Ion-Beam-Amorphized Si, Ge, and GaAs // *Phys. Rev. B.* 2002. V. 65. Art. No. 165329.
30. Cohen C. *et al.* Transformation to Amorphous State of Metals by Ion Implantation: P in Ni // *Phys. Rev. B.* 1985. V. 31. P. 5–14.
31. Bezakova E. *et al.* Implantation-Induced Amorphization of InP Characterized with Perturbed Angular Correlation // *Appl. Phys. Lett.* 1999. V. 75(13). P. 1923–1925.

32. *Zheng P. et al.* Temperature Influence on the Damage Induced Si Implanted InP // *J. Appl. Phys.* 1991. V. 70(2). P. 752–757.
33. *Bench M. W.* Transmission Electron Microscopy Investigation of Ion Implantation Damage in GaAs and Other Semiconductors. Ph.D. Thesis. Univ. of Illinois at Urbana-Champaign, 1992.
34. *Kucheyev S. O.* Amorphous Zone Evolution in Si during Elevated Temperature Ion Bombardment // *Nucl. Instr. Meth. B.* 2001. V. 174(1–2). P. 130–136.
35. *Wendler E. et al.* Temperature and Dose Dependence of Damage Production in Si<sup>+</sup> and Se<sup>+</sup> Implanted InP // *Nucl. Instr. Meth. B.* 1995. V. 106(1–4). P. 303–307.
36. *Wendler E., Opfermann T., Gaiduk P. I.* Ion Mass and Temperature Dependence of Damage Production in Ion Implanted InP // *J. Appl. Phys.* 1997. V. 82(12). P. 5965–5975.

Received on January 13, 2009.